2020 IEEE/RSJ International Conference on Intelligent Robots and Systems (IROS)
October 25-29, 2020, Las Vegas, NV, USA (Virtual)

An External Stabilization Unit for High-Precision Applications of Robot Manipulators

Tobias F. C. Berninger[1], Tomas Slimak[1], Tobias Weber[2] and Daniel J. Rixen[1]

***Abstract*— Because of their large workspace, robot manipulators have the potential to be used for high precision non-contact manufacturing processes, such as laser cutting or welding, on large complex work pieces. However, most industrial manipulators are not able to provide the necessary accuracy requirements. Mainly because of their flexible structures, they are subject to point to point positioning errors and also vibration errors on a smaller scale. The vibration issues are especially hard to deal with. Many published solutions propose to modify the robot's own control system to deal with these problems. However, most modern control techniques require high fidelity models of the underlying system dynamics, which are quite difficult to obtain for robot manipulators. In this work, we propose an external stabilization unit with an additional set of actuators/sensors to stabilize the process tool, similar to Optical Image Stabilization systems. We show that, because of collocated control, a model of the robot's own dynamic behavior is not needed to achieve high tracking accuracy. We also provide testing results of a prototype stabilizing a dummy tool in two degrees of freedom on a UR10 robot, which reduced its tracking error by two orders of magnitude below 20 micrometers.**

I. INTRODUCTION

The ability of robot manipulators to cover a large workspace while also being able to follow complex trajectories has sparked an interest to also utilize them for highly precise, contactless manufacturing processes, like high precision laser cutting or welding. However, depending on the application, most robot manipulators are not able to provide the necessary tracking precision. The main reason for this are unavoidable flexibilities in the gears, joints and links of the robot, as well as typical quality issues like manufacturing tolerances and backlash in the gears. Since most industrial robots are position controlled on the motor side of their joints, they are not able to include these deficiencies in their control loop and rely on simple inverse kinematics to steer the tool center point (TCP) at the tip of the robot along a desired trajectory. Depending on the robot's position, this will cause a positioning error, since the flexible elements of the robot will deform due to its own weight and drop below the desired position. Robot manufacturers offer expensive static calibration methods to somewhat compensate for this [1], however, a much more difficult problem to deal with are dynamic vibrations at the robot's TCP that also deteriorate its tracking performance [2].

This work was supported by Boeing Research & Technology - Europe.

[1]Tobias F. C. Berninger, Tomas Slimak and Daniel J. Rixen are with the Chair of Applied Mechanics, TU Munich, 85748 Garching, Germany t.berninger@tum.de

[2]Tobias Weber is with Boeing Research & Technology - Europe, Brabanterstr. 4, 80805 Munich, Germany Tobias.Weber@boeing.com

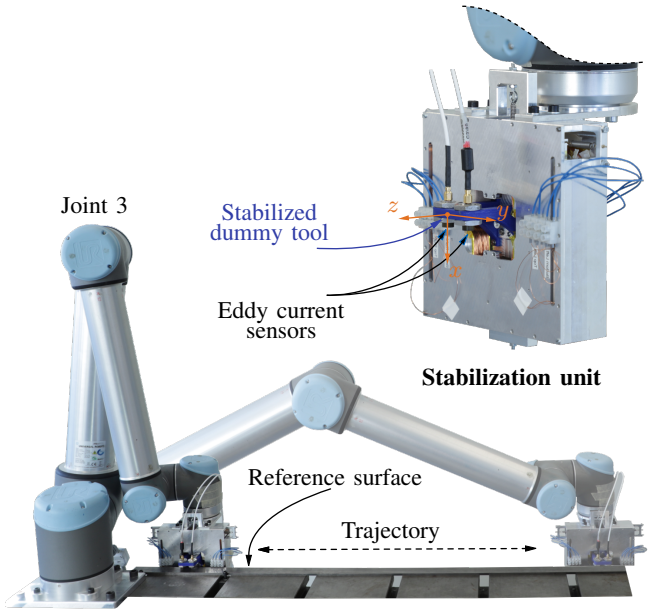

Fig. 1: A UR10 robot performing a horizontal trajectory. An additional stabilization unit is attached to the robot to stabilize a dummy tool.

These vibration problems are mainly caused by the excitation of the robot's structural dynamics due its own motion. Over the past decades, there has been a large effort to reduce these structural vibrations by modifying the robot's own control system. [3–6] consider flexible joints in their control schemes, while [2, 7–9] try to incorporate the dynamic equations of a flexible link. The effects of the combination of both flexible links and joints are investigated more rarely [10–12]. Most of these approaches have in common that they require high quality models of the underlying system dynamics in order to work properly. However, acquiring a high fidelity model of the underlying dynamics is very hard using measurements [13] and even more difficult to predict without having measurements available [14]. This is mainly due to the high number of components, friction inside of the gears [15] and the pose dependent structural dynamics [13].

For this reason, we developed an external approach that does not need a model of the robot's dynamic behavior in order to achieve very high precision. We added a stabilization unit between the robot's mounting flange and the tool with an additional set of actuators and sensors, Fig. 1. As we will show later, this greatly simplifies the underlying control problem, since we can employ control techniques for collocated sensor/actuator pairs. For our application, the goal of

the stabilization unit is to compensate for the deficiencies of the robot by keeping a dummy tool at a desired distance (measured in x-direction) and rotation (around the z-axis) relative to a reference surface.

Stabilized platforms are already used in a range of applications, e.g for beam pointing devices on ships [16] or Optical Image Stabilization (OIS) systems for camera lenses [17]. However, the specific requirements and implementation of the concept vary widely between applications. A similar concept for robot manipulators is the micro/macro approach, which uses a robot with a first set of macro degrees of freedom (DOF) for covering a large workspace and another set of micro DOF at the end with a small workspace that provide the necessary precision [18, 19]. However, this requires the development of a new type of robot manipulator, which also still has to deal with the same vibration issues [20]. The stabilization unit proposed here can simply be attached to any type of industrial robot manipulator, greatly simplifying its use to enhance existing applications. [21] is the most similar published work, however, the vibration isolation is done passively and the author does not provide any testing results on a moving robot.

While the overall design of the proposed stabilization unit is inspired by typical OIS systems, there are a few major differences for our application:

- Instead of stabilizing two translational DOF, we have to stabilize one translational and one rotational DOF.
- Additional to attenuating harmful vibrations, we also have to track a reference to compensate for the slow drift of the robot with $20\,\mu\mathrm{m}$ precision and total displacements of up to $\pm 2.5\,\mathrm{mm}$.
- While we tried to keep the weight as low as possible, we still have to stabilize a mass of $0.2\,\mathrm{kg}$, which is much larger compared to most OIS systems.
- The system must be able to attenuate vibrations up to $50\,\mathrm{Hz}$.

II. DESIGN OF THE STABILIZATION UNIT

In order to stabilize the desired DOF, we mounted the stabilized platform that carries the dummy tool to two sets of two springs each, Fig. 2.d. The two vertical springs are in line with the center of the platform, while the two horizontal springs are off-center. A small translational motion will only be affected by the vertical springs, since the translational motion of the platform is orthogonal to the horizontal springs. In the same way, a rotation of the platform will only be affected by the horizontal springs. This very effectively decouples the two DOF for small motions, which means that we can design each DOF as a single harmonic oscillator separately.

The spring stiffnesses are chosen such that we achieve the same eigenfrequency of $22\,\mathrm{Hz}$ for both DOF respectively. This is a trade-off, since we need high stiffness in order for the mechanical system to be able to hold the stabilized tool passively in place, without the actuators being turned on. However, high stiffnesses also means that we need high actuation forces to move the platform.

In order to block all other DOF, we attached a guide pin to the back of the platform, Fig. 2.b. The pin glides in a linear guide, which is attached to the back plate of the housing (not visible in the figure). This allows the platform to only rotate around the center of the guide pin and move in vertical direction along the linear guide. Attached to the guide pin is a fifth spring that pulls the stabilized platform onto three ceramic balls. Since the spring is again orthogonal to both desired DOF, it does not have to be considered for the dynamics of the system for small motions. The ceramic balls ensure that the platform can only move within the x-y plane, with as little friction as possible.

Since we want to achieve on overall precision of the system in the micrometer range, it is important to stress that a good mechanical design with no slack, as little friction as possible and low tolerances is absolutely essential. Deficiencies in the mechanical design are usually very hard to compensate, even with modern control techniques.

The platform is actuated using two Lorenz actuators designed specifically for this application, Fig. 2.a. The actuators can produce a vertical force on the left and right hand side of the platform separately. Both forces pointing in the same direction will cause the platform to move vertically, while opposite pointing forces will cause it to rotate. One Lorenz actuator consists of four coils, with two coils in front of and two behind the platform, Fig. 2.c. Six magnets are placed within the platform in such a way that the sides of the coils are always covered within the $\pm 2.5\,\mathrm{mm}$ movement range of the platform. Each actuator can produce a peak force of $35\,\mathrm{N}$ and a continuous force of $20\,\mathrm{N}$. Lorentz actuators have the great advantage of applying their force without contact, keeping the overall friction of the system as low as possible.

Finally, there are two eddy-current sensors mounted to the dummy tool, which measure the distance of the left and right corner of the dummy tool to the reference surface.

III. CONTROL DESIGN AND SIMULATION

In order to find a suitable control design for the stabilization unit, we first built a flexible multi-body simulation of the UR10. The simulated robot consists of rigid bodies of the same geometry and density as those of the UR10 and flexible joints. The joint stiffnesses are tuned such that the first three eigenfrequencies and modal damping of the simulated robot approximately match the real one. This is verified using a driving point measurement at the tool center point (TCP) of the robot. A more detailed description about the type of simulation used here can be found in [22] and [12].

We want to stress that we did not aim to exactly replicate the dynamic behavior of the UR10, since this is quite an involved task because of the pose dependent structural dynamics of robot manipulators [13, 14]. However, we wanted to use a robot model that behaved similarly enough to the real robot to design the controller of the stabilization unit, while also being able to test possible interactions between the actuation of the stabilized platform and the robot's own structural dynamics.

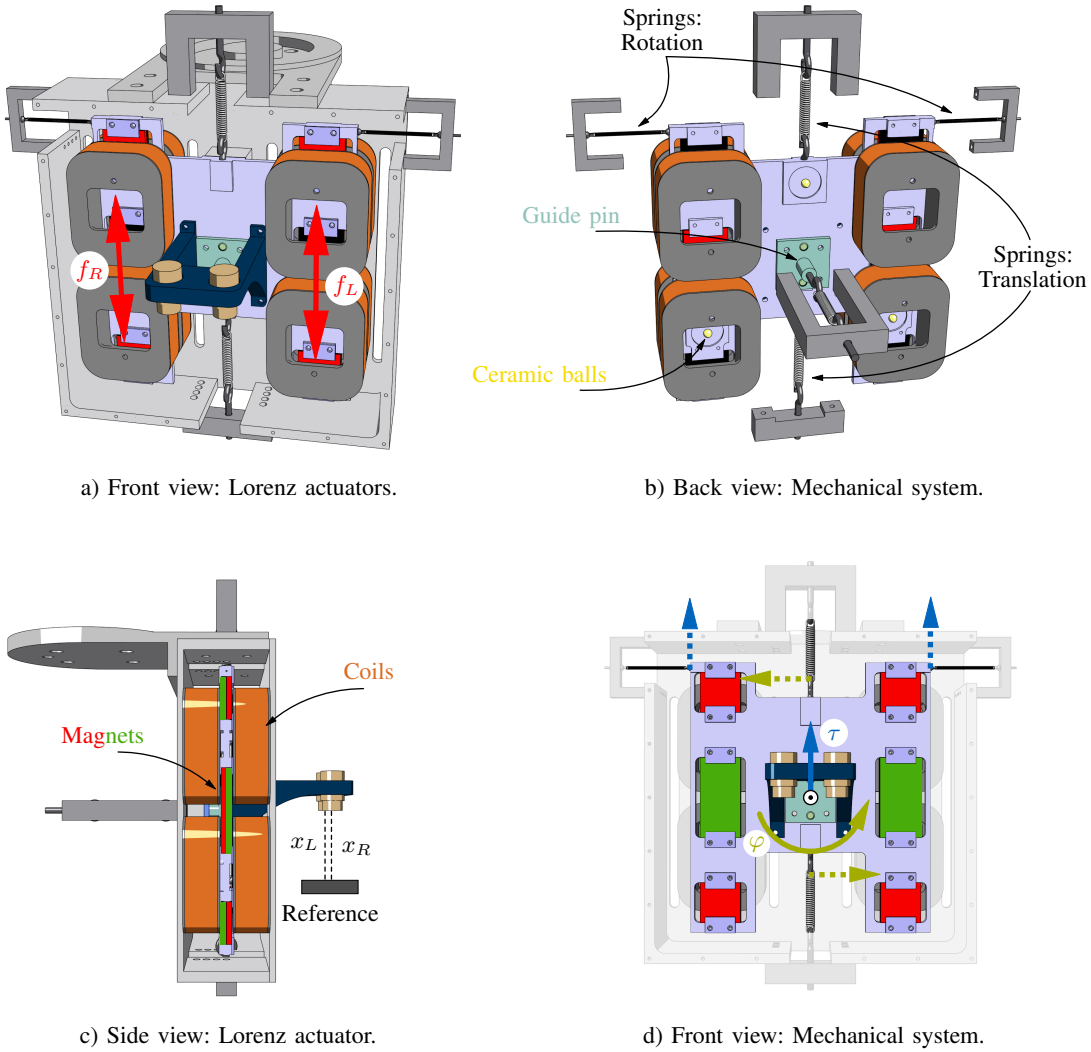

a) Front view: Lorenz actuators.

b) Back view: Mechanical system.

c) Side view: Lorenz actuator.

d) Front view: Mechanical system.

Fig. 2: Mechanical design and Lorenz actuators of the stabilization unit.

The stabilization unit is modeled in the same ways as described in section II and is coupled to the robot's mounting flange.

A. Controller Design

Regarding the control design, we tried many different types of control strategies, however, most of them did not achieve the same performance on the real system as in the simulation. This was mostly due to stability issues caused by sensor noise that limited their possible performance, which caused them to not be able to meet our accuracy requirement of $20\,\mu\mathrm{m}$ tracking precision.

The flow chart of our final control architecture is shown in Fig. 3. The general setup is a stabilizing controller that uses the reference measurements $x_{L/R}$ to keep the translation τ and rotation φ of the stabilized tool at a desired constant value τ_d and φ_d. The controller is implemented on a dSpace MicrolabBox (Fig. 3 blue), which runs with $5\,\mathrm{kHz}$ and produces a desired current $I_{d_{L/R}}$ for the Lorenz actuators. The desired current is sent via an analog connection to two ELMO Solo Whistle motor drivers (Fig. 3 green) that serve as current controllers. Thanks to their high clock rate of $10\,\mathrm{kHz}$, we can achieve a high bandwidth using simple PI-controllers such that the desired currents are practically directly proportional to the actuator forces for our purposes:

$$I_{d_{L/R}} \sim f_{L/R}\ . \tag{1}$$

For this reason, the dynamics of the electrical system was not considered in the following control design.

The stabilizing controller first transforms the measurements of the left x_L and right x_R displacement sensor into the translational τ and rotational φ DOF of the stabilization unit:

$$\begin{bmatrix}\tau\\ \varphi\end{bmatrix} = \underbrace{\begin{bmatrix}0.5 & 0.5\\ 1/d & -1/d\end{bmatrix}}_{\Phi}\begin{bmatrix}x_L\\ x_R\end{bmatrix}\ . \tag{2}$$

under the assumption of small rotations and with d being the distance between the displacement sensors.

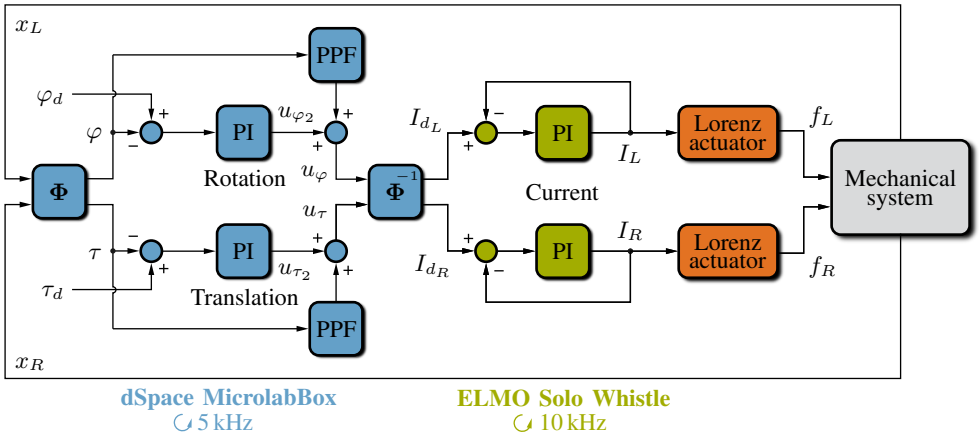

Fig. 3: Flow chart of the stabilization units control structure.

Because of our spring arrangement, as explained in section II, we can now treat each DOF as a single harmonic oscillator. This becomes apparent by looking at the closed-loop transfer function of the translational DOF shown in Fig. 4. The blue curve shows the closed-loop response to a desired translation τ_d for a simple P-controller with very low gain. We can see the eigenfrequency of the actuator at 22 Hz, causing an overall 180 ° phase delay. There is no additional pole caused by the rotational DOF visible in the phase, meaning that both DOF are effectively decoupled. However, we can see a pole-zero pair lying close to each other around 14 Hz. This is caused by the first eigenfrequency of the robot's own structural dynamics.

As already mentioned, the structural dynamics of the robot arm are pose dependent and normally very difficult to deal with using typical joint controllers of the robot. However, since we are using an additional sensor/actuator pair attached to the TCP of the robot we can utilize collocated control. This greatly simplifies the control problem and is the biggest advantage of using an external stabilization device: Using a collocated sensor/actuator pair causes the structural dynamics of the robot to appear as alternating pole-zero pairs in the closed-loop transfer function [23]. Even a simple P-controller will cause the poles to very quickly converge on-top of their respective zeros and effectively cancel out the robot's structural dynamics. The amount of gain needed is determined by the ratio of stabilized mass to the mass of the robot. Our simulation showed that, in the case of the UR10, the interaction between the controller of the stabilization unit and the robot's structural dynamics only have to be considered for a stabilized mass above 10 kg, which is above the maximum payload of the robot and way above our application. This also shows that, although we are only stabilizing 0.2 kg in this work, this approach is easily scalable to heavier pay loads, assuming one can produce the necessary control forces.

Adding an I-part to the controller at this point will cause the system to very quickly become unstable, because of the by design very low damping of the mechanical system. Another way to increase the control bandwidth is to increase

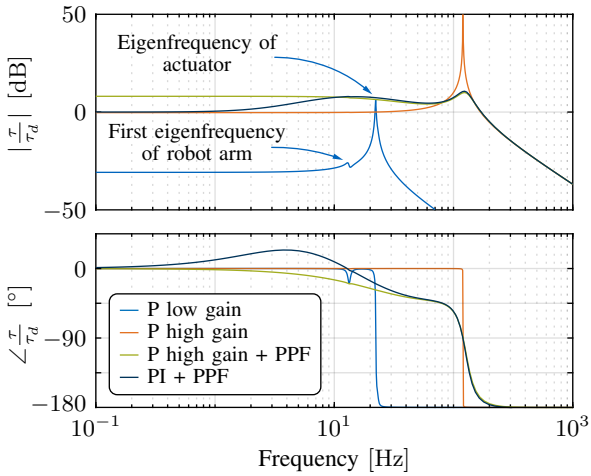

Fig. 4: Closed-loop transfer function of the translational DOF for different controller gains.

the gain of the P-controller. The effect of this on the closed-loop transfer function is shown by the orange curve in Fig. 4. The only pole that is not canceled out is the one caused by the translational springs of the stabilization unit, which is pushed to a higher frequency by the increased gain of the P-controller. As a consequence, we achieve a quite high control bandwidth that is theoretically stable, however, at the cost of a very high resonance peak with even less damping. A system like this is unusable in practice, since it will resonate for multiple seconds in response to even small disturbances and will immediately get unstable because of the large amplification of noise.

In theory, the large resonance peak could be reduced by adding a sufficiently large D-part to the controller. However, the amplification of noise makes this approach unusable, since we would need a large amount of D-gain to achieve the desired tracking precision. Classical control techniques like lead-lag compensation, as well as more modern approaches like pole placement or LQR controllers, improved the system's performance, however, did not achieve the desired tracking precision on the real system.

We finally achieved the desired performance by using a popular Active Vibration Damping control technique known as Positive Position Feedback (PPF), which is used to damp the dynamic response of structures. Since this is essentially the same problem, we can use the same type of controller to damp our closed-loop resonance. The great advantage of these controllers is that they are easy to implement, not sensitive to spillover due to unmodeled system dynamics and are not destabilized by finite actuator dynamics [24]. The transfer function of a PPF controller is:

$$C_{PPF} = \frac{g}{s^2 + 2\zeta_c \omega_c s + \omega_c^2} \tag{3}$$

With g being the gain, ζ_c the damping ratio and ω_c the eigenfrequncy of the PPF controller. The input for the controller is the measured translational DOF τ and the output is connected in parallel to the P-controller, Fig. 3 (denoted with PI, since we will later add an I-part). This is essentially like attaching a virtual tuned mass-damper to the control plant to reduce unwanted vibrations.

The modified control plant P_{τ_m} that the P-controller is now acting on can be calculated using:

$$P_{\tau_m} = \frac{\tau}{u_{\tau_2}} = \frac{P_\tau}{1 - C_{PPF} \cdot P_\tau} \ , \tag{4}$$

with $P_\tau = \tau / u_\tau$ being the original plant of the translational DOF of the mechanical system. Finally, the closed-loop transfer function becomes:

$$G_{\tau_{cl}} = \frac{\tau}{\tau_d} = \frac{C_{PI} \cdot P_{\tau_m}}{1 + C_{PI} \cdot P_{\tau_m}} \tag{5}$$

$$= \frac{C_{PI} \cdot P_\tau}{1 - P_\tau \cdot C_{PPF} + C_{PI} \cdot P_\tau} \tag{6}$$

With C_{PI} being the transfer function of a PI-controller. Equation (6) is plotted in Fig. 4 in green, with the same amount of P gain as before and an the I-part set to zero. The damping ratio of the PPF controller is set to $\zeta_c = 0.5$, the controller eigenfrequency ω_c is set equal to the closed-loop resonance at 120 Hz. The gain of the PPF controller g is increased until a desirable amount of damping is achieved. However, since the PPF controller is essentially a second-order system, this will stack static gain on top of the P-controller and cause the system to overshoot. Since we increased the damping in our system, we can now safely add an I-part to our controller (Fig. 4, dark blue curve), which resolves this problem. We do not need a very large amount to fix the static overshooting, since we are not interested in a very high bandwidth to follow a desired translation τ_d. The goal of the controller is to hold a constant distance to the work peace, while being very robust against external disturbances caused by the robot arm.

Since we decoupled both DOF of the stabilization unit in the beginning, we can use the exact same type of controller for the rotational DOF.

B. Simulation Results

The controller is tested using our flexible multi-body simulation of the UR10. The simulated robot performs the same test as shown in Fig. 1, by moving from a completely retracted position to a stretched out position following a horizontal trajectory. To test the robustness of our controller, we use a strictly linear trajectory that causes high jerk in the beginning of the motion. Additionally, we add an external force that presses on the 3rd joint of the robot after 4 seconds and releases the robot again after 6 seconds.

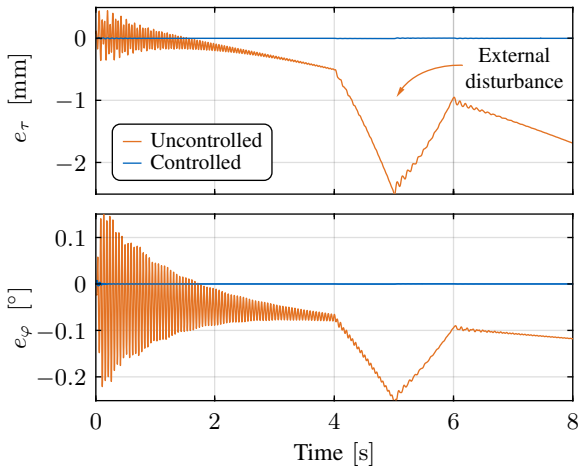

Fig. 5: Translational and rotational error e_τ / e_φ at the TCP of the simulated robot during a horizontal trajectory with an additional disturbance.

The simulation results are depicted in Fig. 5, which shows the translational error e_τ and rotational error e_φ of the stabilized tool at the TCP of the robot. The orange curve shows the errors with the stabilization turned off. The high jerk in the beginning excites the structural dynamics of the robot and causes it to vibrate. The robot tries to follow a horizontal path, however, only the motor positions of the joints are directly controlled, like in most industrial robots. Since the load on the joints increases while the robot is stretching out, the TCP continuously drops below the expected trajectory due to its joint flexibilities. The tool also simultaneously tilts, which is shown in the lower graph. This is made even worse by the external force acting on the 3rd joint of the robot between seconds four and six, which also causes some light vibrations.

The blue curve in Fig. 5 shows the performance of the system with the stabilization turned on. The stabilized tool is almost completely decoupled from the robot's structural dynamics and any other disturbances transmitted by the robot arm. The tracking error is reduced by over two orders of magnitude, with the tool almost perfectly following the desired distance and orientation relative to the reference surface.

This shows the great advantage of using an external stabilization device with additional collocated sensor/actuator pairs at the tip of the robot for high precision applications. Remember, that we do not need a model of the robot's own dynamic behavior in order to acquire this performance boost. Normally, if one would want to achieve a similar precision by

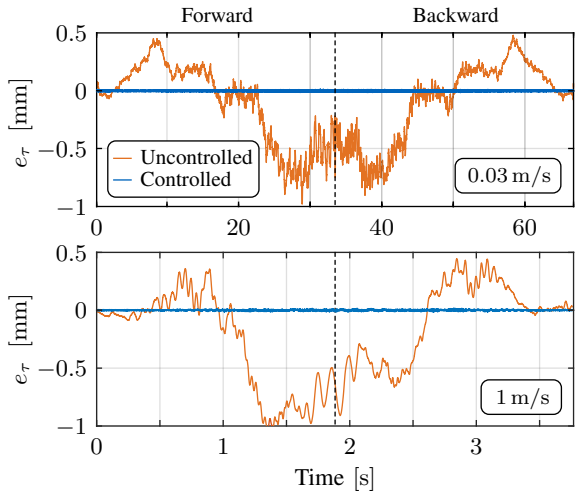

Fig. 6: Measured translational error e_τ at the dummy tool during a horizontal trajectory with two different movement speeds using a UR10 robot.

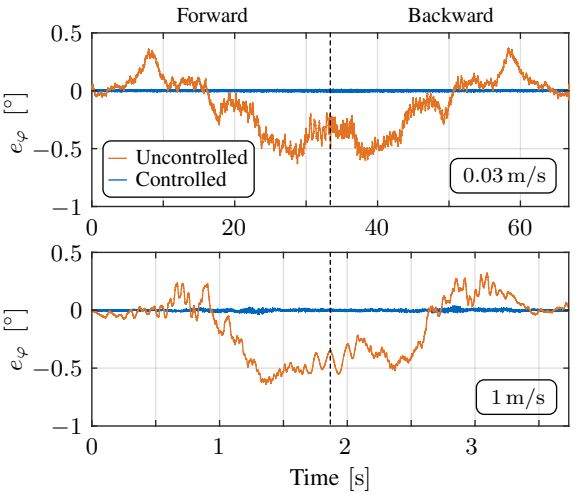

Fig. 7: Measured rotational error e_φ at the dummy tool during a horizontal trajectory with two different movement speeds using a UR10 robot.

modifying the robot's own control system, one would need very precise models of the robot's dynamics that are very difficult to acquire. With this setup, we only had to worry about the actuator dynamics, which we can design ourselves as simple harmonic oscillators.

IV. TESTING RESULTS

To test the stabilization unit, it is mounted to a UR10 robot, Fig. 1. The robot performs the same horizontal trajectory as in the simulation, however, moving forward and backward. To generate a reference measurement, we physically blocked the springs of the stabilization unit. The results are shown in Fig. 6 and 7 in orange. The test is performed with a relatively low trajectory speed of $0.03\,\mathrm{m/s}$ and a fast speed of $1\,\mathrm{m/s}$.

These simple measurements already show why it is so difficult to acquire high fidelity models of robot manipulators: For the semi-static behavior, we expected the robot to continuously drop below the desired trajectory because of its flexible components. However, the TCP of the real robot first starts to slightly raise and then drops while maintaining a constant distance in some sections. This behavior is reproducible, which can also be seen in the upper graph of Fig. 6, which shows the same error profile for moving forwards and backwards.

The vibration behavior is also different from our simulation. This is because the real robot uses a minimum jerk trajectory, which does not cause a high excitation force in the beginning. However, the robot continuously vibrates at different frequencies. This is most likely caused by grinding of the gears that provide a constant, however hard to predict, excitation over all joints.

Nevertheless, we achieve a similar error reduction from the real stabilization unit as in the simulation (Fig. 6 and Fig. 7, blue curve), since the control design is not depending on a prediction of the robot's behavior. Overall, the maximum translational error is reduced from a maximum of $1\,\mathrm{mm}$ to a maximum of $15\,\mu\mathrm{m}$, with similar error reduction for the rotational DOF. The performance of the system is pretty much only limited by the noise floor of the eddy current sensors, which is around $10\,\mu\mathrm{m}$ in operation. The results are also basically independent of the trajectory speed of the robot. The system also proved to be very robust against external disturbances, like a human hitting against the robot during operation, which is shown in the attached video.

V. CONCLUSIONS AND FUTURE WORK

In this work, we have developed and tested an external stabilization unit for high-precision applications of robot manipulators. The mechanical design was inspired by typical OIS systems, however, we had to stabilize one translational and one rotational DOF instead of the typical two translational DOF. We arranged two sets of two springs in such a way that both DOF can be designed as independent single harmonic oscillators. We used a flexible multi-body simulation to show that the dynamic behavior of the robot does not have to be considered in the control loop of the stabilization unit, thanks to the application of collocated sensor/actuator pairs. We only had to control the actuator dynamics of our own system, which was done using PPF controllers. Simulation and testing results on a real UR 10 robot both showed a reduction of the translational and rotational errors by two orders of magnitude.

We are aware that the performance of the system relies on a high quality measurement of the reference surface, which might not be as simple to implement for different applications. For this reason, we will look into integrating additional sensor data (e.g. inertial measurements units, accelerometers, camera systems) into the control loop using sensor fusion, in order to also make this approach work for different applications.

REFERENCES

[1] A. Nubiola and I. A. Bonev, "Absolute calibration of an ABB IRB 1600 robot using a laser tracker", *Robotics and Computer-Integrated Manufacturing*, vol. 29, no. 1, 2013.

[2] W. J. Book, "Controlled motion in an elastic world", *Journal of Dynamic Systems, Measurement, and Control*, vol. 115, no. 2B, 1993.

[3] L. Sweet and M. Good, "Redefinition of the robot motion-control problem", *IEEE Control Systems Magazine*, vol. 5, no. 3, 1985.

[4] H.-B. Kuntze and A. Jacubasch, "Control algorithms for stiffening an elastic industrial robot", *IEEE Journal on Robotics and Automation*, vol. 1, no. 2, 1985.

[5] A. D. Luca and F. Flacco, "A PD-type regulator with exact gravity cancellation for robots with flexible joints", in *2011 IEEE International Conference on Robotics and Automation*, IEEE, 2011.

[6] A. Albu-Schäffer and G. Hirzinger, "A globally stable state feedback controller for flexible joint robots", *Advanced Robotics*, vol. 15, no. 8, 2001.

[7] A. D. Luca and G. D. Giovanni, "Rest-to-rest motion of a one-link flexible arm", in *2001 IEEE/ASME International Conference on Advanced Intelligent Mechatronics.*, IEEE.

[8] R. H. Cannon and E. Schmitz, "Initial experiments on the end-point control of a flexible one-link robot", *The International Journal of Robotics Research*, vol. 3, no. 3, 1984.

[9] B. K. Post, "Robust state estimation for the control of flexible robotic manipulators", PhD thesis, Georgia Institute of Technology, 2013.

[10] J. Ohr *et al.*, "Identification of Flexibility Parameters of 6-axis Industrial Manipulator Models", in *ISMA 2006*, 2006.

[11] F. Behi and D. Tesar, "Parametric identification for industrial manipulators using experimental modal analysis", *IEEE Transactions on Robotics and Automation*, vol. 7, no. 5, 1991.

[12] T. Berninger, M. Ochsenius, and D. Rixen, "Evaluation of an external vibration damping approach for robot manipulators using a flexible multi body simulation", in *IEEE/ASME International Conference on Advanced Intelligent Mechatronics, AIM*, 2019.

[13] T. F. C. Berninger, S. Fuderer, and D. J. Rixen, "Modal analysis of a 7 DoF sweet pepper harvesting robot", in *Topics in Modal Analysis & Testing, Volume 8*, Springer International Publishing, 2019.

[14] S. A. Zimmermann *et al.*, "Dynamic modeling of robotic manipulators for accuracy evaluation", in *IEEE-RAS International Conference on Robotics and Automation*, 2020.

[15] J. Baur *et al.*, "Experimental friction identification in robot drives", in *2014 IEEE International Conference on Robotics and Automation (ICRA)*, IEEE, 2014.

[16] J. M. Hilkert, "Inertially Stabilized Platform Technology Concepts and Principles", *IEEE Control Systems*, vol. 28, no. 1, 2008.

[17] B. Cardani, "Optical image stabilization for digital cameras", *IEEE Control Systems*, vol. 26, no. 2, 2006.

[18] W. J. Book and S. H. Lee, "Vibration control of a large flexible manipulator by a small robotic arm", in *1989 American Control Conference*, IEEE, 1989.

[19] W. Book and J. Loper, "Inverse dynamics for commanding micromanipulator inertial forces to damp macromanipulator vibration", in *Proceedings 1999 IEEE/RSJ International Conference on Intelligent Robots and Systems. Human and Environment Friendly Robots with High Intelligence and Emotional Quotients (Cat. No.99CH36289)*, IEEE.

[20] I. Sharf, "Active damping of a large flexible manipulator with a short-reach robot", *Journal of Dynamic Systems, Measurement, and Control*, vol. 118, no. 4, 1996.

[21] R. Deng, "Integrated 6-dof lorentz actuator with gravity compensation for vibration isolation in in-line surface metrology", PhD thesis, TU Delft, 2017.

[22] T. F. C. Berninger *et al.*, "The Influence of Structural Dynamics on Cascaded Joint Position Control of a Flexible Beam with a Compliant Gear", in *IEEE-RAS International Conference on Control, Automation and Systems*, 2019.

[23] A. Preumont, *Vibration Control of Active Structures: An Introduction*. Springer, 2002.

[24] J. L. FANSON and T. K. CAUGHEY, "Positive position feedback control for large space structures", *AIAA Journal*, vol. 28, no. 4, 1990.